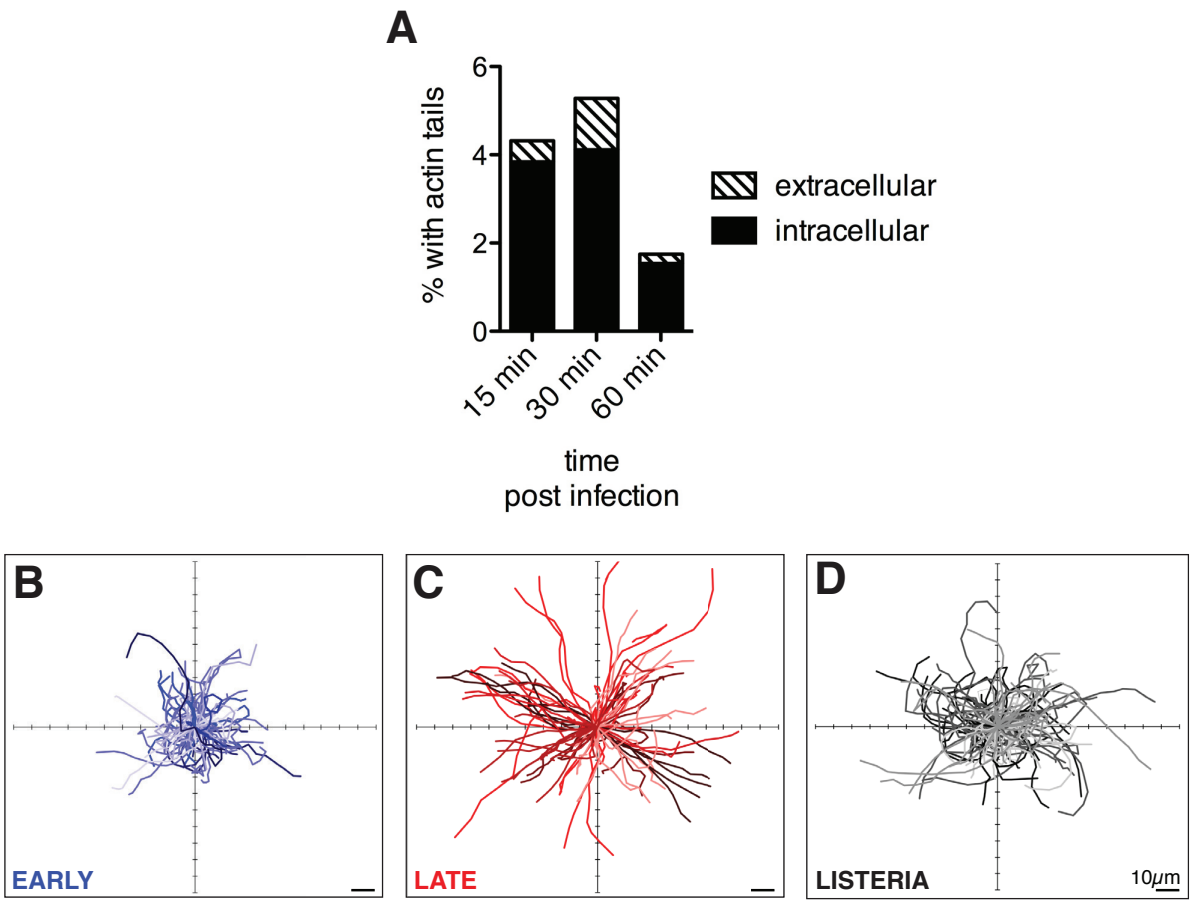

Figure S1, related to Figure 1 – Quantification of intracellular versus extracellular bacterial localization and tracks of motility paths.

(A) Graph showing the percentage of bacteria with actin tails, and the proportion of these that were intracellular (black bar) versus extracellular (hashed bar). For these studies, HMEC-1 cells were infected with wild type *R. parkeri* for 0-30 min. They were fixed and stained to differentiate intracellular and extracellular bacteria as described previously [S1], and imaged to quantify intracellular or extracellular localization as well as actin tail association in 10 random fields of view over two independent experiments performed in duplicate. **(B-D)** X-Y plots of bacterial movement paths over 60 s, with start position defined as (0,0), for individual *R. parkeri* **(B)** early or **(C)** late, or of **(D)** *L. monocytogenes*. Each path is shaded uniquely.

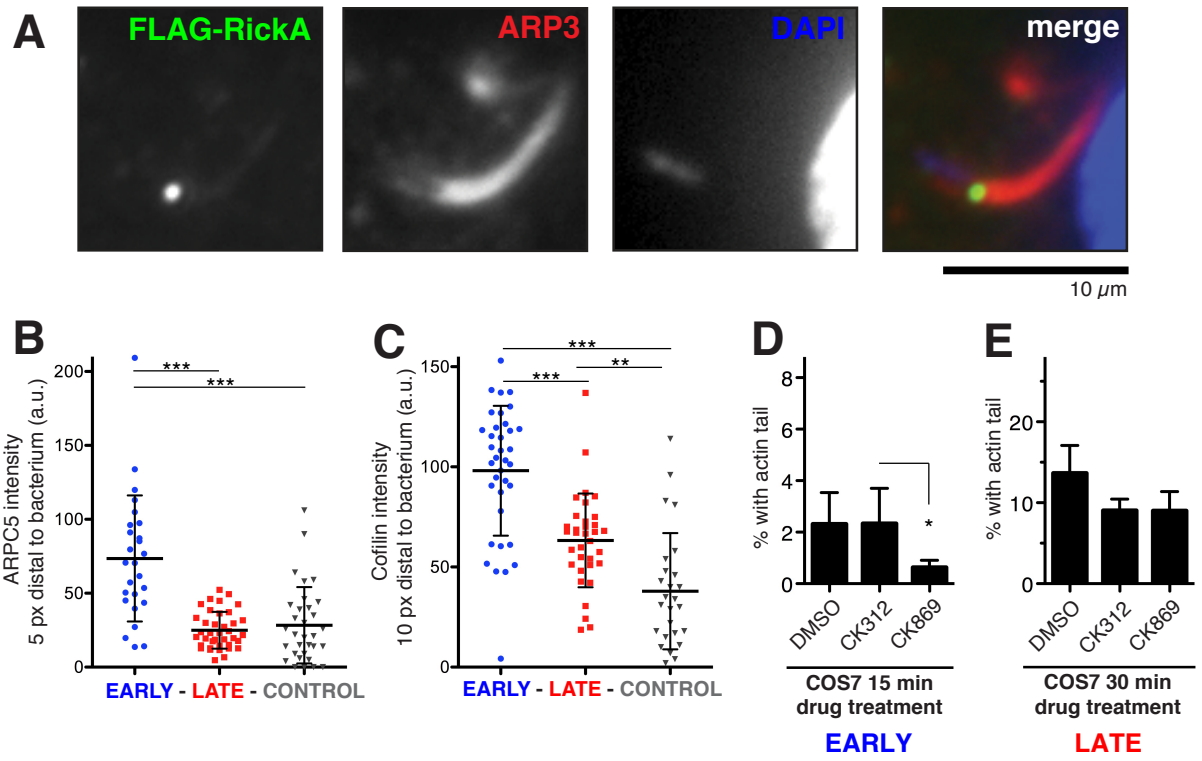

Figure S2, related to Figure 2 - Different host proteins are recruited and required for early and late motility.

(A) Arp3 protein localization in Vero cells infected with FLAG-RickA expressing *R. parkeri* [S2] for 30 min, fixed and stained with anti-Arp3 antibody (red) [S3], anti-FLAG M2 antibody (green) and DAPI to label DNA (blue). **(B)** ARPC5 intensity at 5 pixels distal to each bacterium, as in Figure 2D-F. **(C)** Cofilin intensity at 10 pixels distal to each bacterium, as in Figure 2A-C. For (B, C), data is expressed as mean ± SD, with ** $p<0.01$ and *** $p<0.001$ indicating means vary significantly by ANOVA with Bonferroni's Multiple Comparison Test. Control measurements were taken along 100 pixel lines in adjacent areas of the cell without actin tails. a.u. = arbitrary units. **(D)** Percent of all bacteria with an actin tail in COS7 cells infected with *R. parkeri* for 15 min to allow invasion, then treated with 1% DMSO or 100 μM inactive control (CK312) or Arp2/3 inhibitor (CK869) for 15 mpi, before fixation at 30 mpi. **(E)** Percent of all bacteria with an actin tail in COS7 cells infected with *R. parkeri* for 48 h, then treated with 1% DMSO or 100 μM CK312 or CK869 for 30 min before fixation. For (D, E) cells were stained with Alexa Fluor 488-phalloidin and anti-*Rickettsia* antibody, and 5-10 random fields of view were imaged. Results are the mean ± SD of three independent experiments performed in duplicate, with * $p<0.05$ indicating means vary significantly by ANOVA with Bonferroni's Multiple Comparison Test.

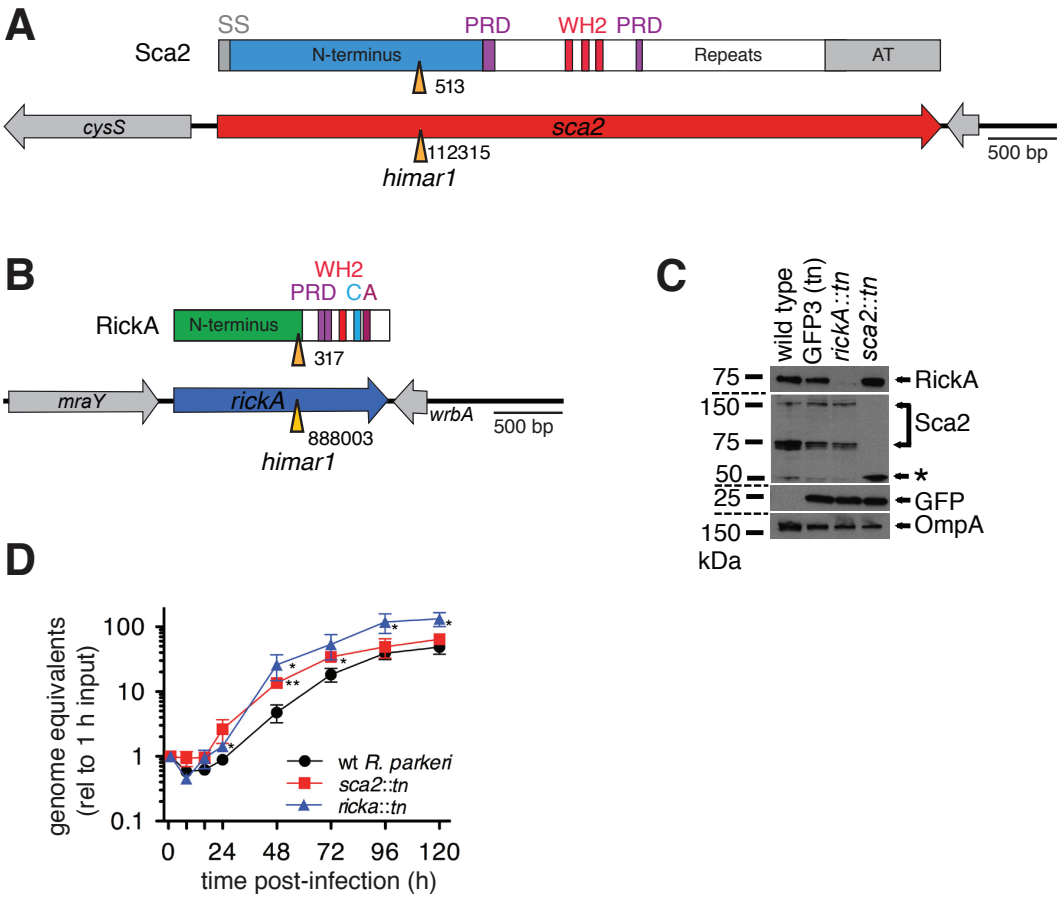

Figure S3, related to Figure 3 – Schematics of transposon insertion mutations.

(A) Schematics of the *sca2* gene in *R. parkeri* and the corresponding Sca2 protein. **(B)** Schematics of the *rickA* gene in *R. parkeri* and the corresponding RickA protein. For (A, B): SS = signal sequence; PRD = proline-rich domain; WH2 = WASP homology 2 domain; AT = autotransporter domain; C = central motif; A = acidic motif. The locations of *himar1* transposon insertions are indicated with yellow arrowheads, along with the predicted amino acid position in the proteins and base pair position in the genome. **(C)** Western blot showing RickA, Sca2, and GFP expression in wild-type *R. parkeri*, a control Himar1 transposon insertion strain (GFP3) [S2], as well as *rickA::tn* and *sca2::tn* strains. The outer membrane protein OmpA was used as a loading control. *, truncated Sca2 fragment expressed in the *sca2::tn* strain. **(D)** One-step growth curve in Vero cells, measuring *Rickettsia* genome equivalents by qPCR using primers to the 17kD antigen gene, relative to a standard curve of 17kD gene DNA [S4], and normalized to input bacteria at 1 hpi. Data are the mean ± SEM from two experiments, each in duplicate, with *p<0.05 or ** p<0.01 indicating the mean varies significantly from wild type at a given time point by unpaired t-test. Variance between curves was not significant.

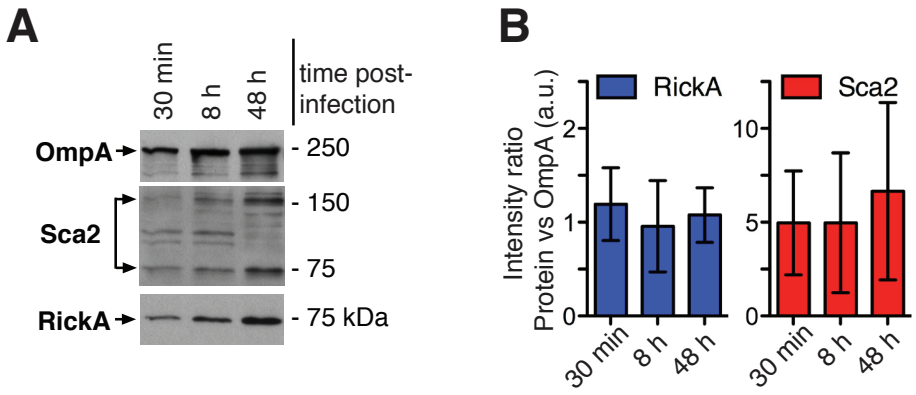

Figure S4, related to Figure 4 – RickA and Sca2 protein levels over time.

(A) Western blot showing Sca2, RickA and OmpA protein levels in HMEC cells infected with wild-type *R. parkeri* for the indicated times post infection; equal amounts of total protein (host + bacteria) were loaded in each lane, but bacterial protein levels increase as they replicate. **(B)** Quantification of protein levels in (A) by densitometry using ImageJ (a.u. = arbitrary units). Major species near 250kD (OmpA), 75kD (RickA) and 150kD+75kD (Sca2) were measured and data are represented as mean ± SEM relative to OmpA loading control in two independent experiments, each with duplicate infection samples. Differences between timepoints are not statistically significant. See also Table S1.

Supplemental Movie Legends

Movie S1, related to Figure 1

Time-lapse spinning disk confocal microscopy of live HMEC-1 cells transfected with EGFP-Lifeact (green) and infected for 20 min with *R. parkeri* expressing mCherry (red). Frames were imaged every 5 s and movie plays at 10 frames/s (50x actual speed). Timestamp min:sec.

Movie S2, related to Figure 1

Time-lapse spinning disk confocal microscopy of live HMEC-1 cells transfected with EGFP-Lifeact (green) and infected for 48 h with *R. parkeri* expressing mCherry (red). Frames were imaged every 5 s and movie plays at 10 frames/s (50x actual speed). Timestamp min:sec.

Movie S3, related to Figure 1

Time-lapse spinning disk confocal microscopy of live HMEC-1 cells stably expressing mCherry-Lifeact (green) and infected for 9 h with *L. monocytogenes* 10403S expressing EGFP (red). Frames were imaged every 5 s and movie plays at 10 frames/s (50x actual speed). Timestamp min:sec.

Table S1: RickA and Sca2 localization patterns during *R. parkeri* infection

RickA				
time post infection (number counted)	RickA localization pattern	% of bacteria with actin tail and pattern	% of bacteria with actin cloud and pattern	% of bacteria without actin and pattern
30 min (n = 1229)	polar	6.8	0.6	1.3
	punctate	0.3	5.3	4.7
	diffuse	0	0.4	4.1
	absent	0	0.7	75.9
8 h (n = 518)	polar	0	0.4	1.2
	punctate	0	0.4	5.8
	diffuse	0.2	0	6.4
	absent	6.2	4.1	75.5
48 h (n = 684)	polar	1.3	0	0
	punctate	0.7	2.3	0.6
	diffuse	4.5	3.2	6.4
	absent	17.4	17.1	46.3
Sca2				
time post infection (number counted)	Sca2 localization pattern	% of bacteria with actin tail and pattern	% of bacteria with actin cloud and pattern	% of bacteria without actin and pattern
30 min (n = 937)	polar	0.3	1.2	1.4
	bipolar	0	0.6	1.6
	diffuse	1.8	2.3	16.3
	absent	6.0	7.0	61.4
8 h (n = 417)	polar	8.6	10.1	9.1
	bipolar	1.7	3.8	2.2
	diffuse	0.2	0.2	16.8
	absent	0.2	0	47.0
48 h (n = 710)	polar	18.9	17.7	30.4
	bipolar	0.6	4.5	4.8
	diffuse	0.1	0.3	3.8
	absent	0.6	0	18.3

Table values indicate the percentage of bacteria with both a given RickA or Sca2 localization pattern and a given actin association pattern at each time point.

Supplemental Experimental Procedures

Antibodies

Antibodies were obtained from the following sources: mouse anti-FLAG M2 monoclonal antibody (Sigma-Aldrich); rabbit anti-Arp3 [S3]; mouse anti-β-catenin (BD Biosciences); rabbit anti-RickA [S5]; rabbit anti-Sca2 [S6]; mouse anti-OmpA M13-3, and mouse anti-*Rickettsia* M14-13 (provided by T. Hackstadt, NIH/NIAID Rocky Mountain Laboratories) [S7]; horseradish peroxidase conjugated anti-mouse and anti-rabbit secondary antibodies for immunoblotting (GE Healthcare); AMCA-, Alexa Fluor 488-, and Alexa Fluor 568-conjugated anti-rabbit and anti-mouse secondary antibodies for immunofluorescence (Invitrogen Molecular Probes).

Plasmids

To generate the plasmid pmCherry-ARPC5, the *Homo sapiens* ARPC5 cDNA was amplified by PCR with HindIII and XbaI restriction sites and ligated into a pmCherry-C1 vector [S8], resulting in a plasmid expressing mCherry fused to the N-terminus of ARPC5 (mCherry-ARPC5). The Lifeact [S9] expression plasmids, including pLifeact-GFP [S10], pLifeact-mCherry [S1] and pLifeact-3xBFP [S11], were described previously. pCLIP2B-Lifeact-mCherry and pCLIP2B-Lifeact-3XBFP were constructed from pCLIP2B, derived from pCLIP [S12]. pCLIP2B and packaging vectors pCMV-VSVg and pCL-SIN-Ampho were gifts from J. Pomerantz (Johns Hopkins University School of Medicine). pEGFP-C2-cofilin (provided by H. Mannherz, Ruhr University) was described previously [S13].

Bacterial strains, growth and purification

Rickettsia parkeri Portsmouth strain was a gift from C. Paddock (Centers for Disease Control and Prevention). *R. parkeri* clonal strains GFPUV-3 [S1], 3XmCherry-2 [S2] and FLAG-RickA-2

[S2] were previously described. *Listeria monocytogenes* strain 10403S and GFP-expressing *L. monocytogenes* [S14] were gifts from D. Portnoy (University of California, Berkeley). *R. parkeri* strains were propagated, transformed, and purified as described previously [S1, S15], with the exception that MD-76R (Merry X-Ray) was substituted for Renografin. *L. monocytogenes* was grown in liquid brain heart infusion (BHI; Difco) for 16 h at 37°C without agitation.

Isolation and characterization of *R. parkeri* with transposon insertions

Strains Sp2 (*sca2::tn*) and Sp34 (*rickA::tn*) were generated in separate experiments by harvesting a 75 cm^2 flask of African green monkey kidney epithelial Vero cells infected with *R. parkeri*, lysing cells by passage through a syringe, washing in 250 mM sucrose, and electroporating with 1 µg of plasmid PMW1650 [S16] at 2.5 kV, 200 ohms, 25 µF, for 5 ms using a Gene Pulser Xcell (Bio-Rad). Bacteria were immediately suspended in 1.4-2.4 µl BHI media, and used to infect wells in 6-well plates of confluent Vero cells with an overlay of Dulbecco's modified Eagle's medium (DMEM) with 2% fetal bovine serum (FBS) and 0.5% agarose. Cells were grown overnight at 34˚C, 5% CO_2, and after 20 h an additional overlay containing 500 ng/ml rifampicin was added for a final concentration of 200 ng/ml rifampicin (Sigma). Selection with 200 ng/ml rifampicin was continued for all subsequent growth. After 6-8 d, plaques were visible in the cell monolayer. Plaques were isolated and expanded in individual wells of Vero cells growing in 6-well plates, and insertion sites were amplified for sequencing using semi-random nested PCR with primers

Ex Tn1 5'-CACCAATTGCTAAATTAGCTTTAGTTCC-3' or

ExTn2 5'-GTGAGCTATGAGAAAGCGCCACGC-3' with

Univ1 5'-GCTAGCGGCCGCACTAGTCGANNNNNNNNNNCTTCT-3'

and primers

InTn1 5'-GCTAGCGGCCGCGGTCCTTGTACTTGTTTATAATTATCATGAG-3' or

InTn2 5'-GCTAGCGGCCGCCCTGGTATCTTTATAGTCCTGTCGG-3' with

Univ2 5'-GCTAGCGGCCGCACTAGTCGA-3'. PCR products were cleaned using ExoSAP-IT (Affymetrix), and sequenced using primers SR095 5'-CGCCACCTCTGACTTGAGCGTCG-3' and SR096 5'-CCATATGAAAACACTCCAAAAAAC-3'. Following sequencing, strains were expanded and plaque purified as described previously [S17] and re-sequenced. Genomic locations were determined using BLAST against the *Rickettsia parkeri* strain Portsmouth genome (GenBank/NCBI accession NC_017044.1).

Cell growth and transfections

African green monkey kidney fibroblast COS-7 cells and epithelial Vero cells, as well as human A549 cells, were obtained from the University of California, Berkeley tissue culture facility. HMEC-1 [S18] cells were obtained from the Centers for Disease Control, Biological Products Branch. Polyclonal HMEC-1 cell lines stably expressing Lifeact-mCherry or Lifeact-3XBFP were generated by retroviral transduction using pCLIP2B plasmids, pCMV-VSVg, and pCL-SIN-Ampho to package virus in HEK293T cells, as described previously [S19]. Cells were selected using 2.5 µg/ml puromycin (EMD Millipore), and sorted for strong fluorescent protein expression using a Cytopeia INFLUX Sorter (UC Berkeley Flow Cytometry Facility). Cells were propagated and transfected as previously described [S1], using 250-500 ng of plasmid DNA and Lipofectamine 2000 (Invitrogen). Imaging or fixation was at 48-72 h post-transfection.

Bacterial infections

For *R. parkeri* infections, HMEC-1 cells were seeded either onto glass coverslips in 24-well plates, glass-bottom dishes (Maktek), or 6-well dishes at approximately 50% cell density. For imaging, cells were infected with *R. parkeri* at ~$1.5x10^5$ pfu/well for 48 h, ~$3x10^5$ pfu/well for 24 h or ~$6x10^5$ pfu/well for less than 24 h. *R. parkeri* were added directly to culture medium, plates were centrifuged at 200 X g for 5 min at 22-25ºC and incubated at 37˚C for short infection times (5 min – 2 h) or 33˚C for longer infections (8 h – 48 h). For growth curves and

immunobloting analyses, infected cells were rinsed three times in phosphate buffered saline (PBS) at 1 h post infection to remove non-adherent bacteria.

For *L. monocytogenes* infections of HMEC-1 cells, overnight cultures of GFP-expressing bacteria were diluted 1:40 in HMEC-1 growth medium and incubated at 37˚C for 15 min, then added to culture dishes at an MOI of 100 and incubated for 1 h at 37˚C with 5% CO_2. Extracellular *Listeria* were rinsed away with PBS, and cells were maintained in HMEC growth medium containing 10 μg/ml gentamicin.

For drug treatments, CK-312 or CK-869 (EMD Chemicals) were diluted in culture medium in 1% DMSO for a final concentration of 100 μM, warmed to 37˚C and used to replace medium at the indicated times post infection. For 30 min treatments, drugs were prepared at 2X concentration and added directly to infected cells.

To measure infectious focus size, 2 x 10^5 A549 cells were plated onto 12 mm^2 coverslips 24 h before infection. *R. parkeri* were added directly to culture medium at an MOI of 0.01, and plates were centrifuged at 200 x g for 5 min at 25ºC and incubated at 33˚C for 1 h. Infected cells were then washed 3 times with PBS before adding DMEM + 10% FBS + 50 μg/ml gentamicin and incubating at 33˚C for 24 h until fixation and staining. To quantify spread, 10 individual infectious foci were imaged and the number of infected cells per focus was calculated. Plaque assays were performed as described previously [S20]. For plaque size measurements, wells were overlaid in PBS with 0.5% agarose and 2% neutral red (Sigma) for a final concentration of 1% dye, incubated overnight at 33˚C and photographed using an AlphaInnotech AlphaImager EP (ProteinSimple).

Immunoblotting and immunofluorescence staining

For Figure 3A, bacteria purified by density gradient centrifugation or syringe lysis were boiled in Laemmli sample buffer. For Figure 4G, infected cells were collected by scraping, lysed using RIPA buffer (50 mM Tris pH 7.6, 150 mM NaCl, 1 mM EDTA, 1% Triton X-100, 0.1% SDS plus

10 mg/ml of aprotinin, leupeptin, pepstatin and chymostatin, and 1 mM PMSF), and boiled in Laemmli sample buffer. Membranes were blocked with 5% dry milk in PBS, probed with primary followed by secondary antibodies, and visualized with ECL detection reagents (GE Healthcare).

For immunofluorescence staining, cells were fixed with 2.5% formaldehyde in PBS at room temperature for 15 min or in –20˚C methanol for 5 min (Figure S2A only), then permeabilized in PBS with 0.5% Triton X-100 for 5 min. Antibodies were diluted in PBS with 2% bovine serum albumin (BSA) and staining was carried out at room temperature using standard procedures, with three exceptions. For intracellular/extracellular staining of bacteria (Figure S1 only), anti-*Rickettsia* staining was performed as described previously [S1]. For anti-RickA and anti-Sca2 staining, coverslips were blocked for 1 h in PBS, 2% BSA, 2% normal goat serum, and primary antibody incubation was at 37˚C. For anti-Arp3 staining (Figure S2A), coverslips were blocked in PBS, 2% BSA, 2% dry milk for 30 min prior to staining. To visualize actin and DNA, 4 U/µl of Alexa Fluor 488 or 568-conjugated phalloidin and/or DAPI (Invitrogen) were included with the secondary antibody. Coverslips were mounted with Prolong Gold anti-fade (Invitrogen), sealed, and stored at 4˚C.

Imaging and analysis

Confocal and timelapse images of live and fixed cells were captured using a Nikon Ti Eclipse microscope equipped with a Yokogawa CSU-XI spinning confocal disc, 60X or 100X (1.4 NA) Plan Apo objectives and a Clara Interline CCD camera (Figures 2, 3E, 4 and Movies S1-S3). Wide-field images were captured using a Nikon Eclipse Ti equipped with a 60X or 100X (1.49 NA) TIRF objective and an Andor Clara Interline CCD camera (Figures 1, 3A and 3C), a Nikon TE 2000 with a 100X (1.4 NA) Plan Apo objective and an ORCA-ER Hamamatsu CCD camera (Figure 2H), or an Olympus IX71 microscope equipped with a 100X (1.35 NA) PlanApo objective lens and a Photometrics CoolSNAP HQ camera (Figure S2A).

Fixed and live-cell images were captured in the TIFF 16-bit format using MetaMorph software (Molecular Devices) or Micro-Manager Software (http://www.micro-manager.org) and then processed to 8-bit files, cropped, adjusted for brightness/contrast, and assembled using ImageJ and Adobe Photoshop. ImageJ was used to track bacterial motility (manual tracking, http://rsbweb.nih.gov/ij/plugins/track/track.html), measure actin tails and plaque sizes (segmented line and measure tools) and quantify bacterial association with actin and protein (threshold tool and cell counter plugin, http://rsbweb.nih.gov/ij/plugins/cell-counter.html). For actin tail morphology scoring, a curved tail had one or more 60-90° changes in direction. A short tail was less than twice the length of its associated bacterium. For actin tail length and intensity quantification, measurements were made on tails of all shapes and sizes using a segmented line tool to follow the entire long axis of the actin tail. For Figure 1C-G and Figure S1B-D, 50-100 bacteria were tracked, and 27-100 tails were measured for each of 12 frames (60 s) from movies collected in at least three separate experiments. For actin tail quantification (Figures 1A, 2G-I, 3B and D, S2D and E) an average of 400 bacteria (range: 76-2140) and 25 host cells were counted per experimental sample. For Figure 4 and Table S1, 10 fields of view containing at least one bacterium visibly expressing each protein were collected as confocal stacks, and maximum intensity projections of each stack were identically processed using ImageJ.

Average cosines of the change in tangent angle between adjacent track segments ($\cos(\Delta\theta)$) were calculated using a custom script in Matlab to analyze the x-y coordinates of each track**.** Average efficiency of movement was calculated by dividing the net x-y displacement by the total path distance over 60 s for each individual bacterium. All data were analyzed using Microsoft Excel or Prism v5.0 (Graphpad Software).

Supplemental References

S1. Reed, S. C. O., Serio, A. W., and Welch, M. D. (2012). Rickettsia parkeri invasion of diverse host cells involves an Arp2/3 complex, WAVE complex and Rho-family GTPase-dependent pathway. Cell. Microbiol. *14*, 529–545.

S2. Welch, M. D., Reed, S. C., Lamason, R. L., and Serio, A. W. (2012). Expression of an epitope-Tagged virulence protein in Rickettsia parkeri using transposon insertion. PLoS ONE *7*, e37310.

S3. Welch, M. D., Iwamatsu, A., and Mitchison, T. J. (1997). Actin polymerization is induced by Arp2/3 protein complex at the surface of Listeria monocytogenes. Nature *385*, 265–269.

S4. Grasperge, B. J., Reif, K. E., Morgan, T. D., Sunyakumthorn, P., Bynog, J., Paddock, C. D., and Macaluso, K. R. (2012). Susceptibility of inbred mice to Rickettsia parkeri. Infect. Immun. *80*, 1846–1852.

S5. Jeng, R. L., Goley, E. D., D'Alessio, J. A., Chaga, O. Y., Svitkina, T. M., Borisy, G. G., Heinzen, R. A., and Welch, M. D. (2004). A Rickettsia WASP-like protein activates the Arp2/3 complex and mediates actin-based motility. Cell. Microbiol. *6*, 761–769.

S6. Haglund, C. M., Choe, J. E., Skau, C. T., Kovar, D. R., and Welch, M. D. (2010). Rickettsia Sca2 is a bacterial formin-like mediator of actin-based motility. Nat. Cell Biol. *12*, 1057–1063.

S7. Anacker, R. L., Mann, R. E., and Gonzales, C. (1987). Reactivity of monoclonal antibodies to Rickettsia rickettsii with spotted fever and typhus group rickettsiae. J. Clin. Microbiol. *25*, 167–171.

S8. Campellone, K. G., Webb, N. J., Znameroski, E. A., and Welch, M. D. (2008). WHAMM is an Arp2/3 complex activator that binds microtubules and functions in ER to Golgi transport. Cell *134*, 148–161.

S9. Riedl, J., Crevenna, A. H., Kessenbrock, K., Yu, J. H., Neukirchen, D., Bista, M., Bradke, F., Jenne, D., Holak, T. A., Werb, Z., et al. (2008). Lifeact: a versatile marker to visualize F-actin. Nat. Methods *5*, 605–607.

S10. Serio, A. W., Jeng, R. L., Haglund, C. M., Reed, S. C., and Welch, M. D. (2010). Defining a core set of actin cytoskeletal proteins critical for actin-based motility of Rickettsia. Cell Host Microbe *7*, 388–398.

S11. Duleh, S. N., and Welch, M. D. (2012). Regulation of integrin trafficking, cell adhesion, and cell migration by WASH and the Arp2/3 complex. Cytoskeleton *69*, 1047–1058.

S12. Pomerantz, J. L., Denny, E. M., and Baltimore, D. (2002). CARD11 mediates factor-specific activation of NF-kappaB by the T cell receptor complex. EMBO J. *21*, 5184–5194.

S13. Mannherz, H. G., Gonsior, S. M., Gremm, D., Wu, X., Pope, B. J., and Weeds, A. G. (2005). Activated cofilin colocalises with Arp2/3 complex in apoptotic blebs during programmed cell death. Eur. J. Cell Biol. *84*, 503–515.

S14. Shen, A., and Higgins, D. E. (2005). The 5' untranslated region-mediated enhancement of intracellular listeriolysin O production is required for Listeria monocytogenes pathogenicity. Mol. Microbiol. *57*, 1460–1473.

S15. Hackstadt, T., Messer, R., Cieplak, W., and Peacock, M. G. (1992). Evidence for proteolytic cleavage of the 120-kilodalton outer membrane protein of rickettsiae: identification of an avirulent mutant deficient in processing. Infect. Immun. *60*, 159–165.

S16. Liu, Z.-M., Tucker, A. M., Driskell, L. O., and Wood, D. O. (2007). Mariner-based transposon mutagenesis of Rickettsia prowazekii. Appl. Environ. Microbiol. *73*, 6644–6649.

S17. Clark, T. R., Ellison, D. W., Kleba, B., and Hackstadt, T. (2011). Complementation of Rickettsia rickettsii RelA/SpoT restores a nonlytic plaque phenotype. Infect. Immun. *79*, 1631–1637.

S18. Ades, E. W., Candal, F. J., Swerlick, R. A., George, V. G., Summers, S., Bosse, D. C., and Lawley, T. J. (1992). HMEC-1: establishment of an immortalized human microvascular endothelial cell line. J. Invest. Dermatol. *99*, 683–690.

S19. Lamason, R. L., Kupfer, A., and Pomerantz, J. L. (2010). The dynamic distribution of CARD11 at the immunological synapse is regulated by the inhibitory kinesin GAKIN. Mol. Cell *40*, 798–809.

S20. Cory, J., Yunker, C. E., Ormsbee, R. A., Peacock, M., Meibos, H., and Tallent, G. (1974). Plaque assay of rickettsiae in a mammalian cell line. Appl. Microbiol. *27*, 1157–1161.